Food Research International 221 (2025) 117190

Contents lists available at ScienceDirect

Food Research International

journal homepage: www.elsevier.com/locate/foodres

Shear stress adaptation of *Listeria monocytogenes* in mono and dual-species biofilms

Krisha Pant *, Jon Palmer, Steve Flint

School of Natural Sciences and Food Technology, Massey University, Palmerston North 4442, New Zealand

ARTICLE INFO

Keywords:
Filaments
Motility
Adhesion
Knitted biofilm
Gene expression

ABSTRACT

While the impact of stress on L. *monocytogenes* associated with food processing has been recognized in planktonic conditions, the available research overlooks the response of this pathogen in the multi-species biofilm, commonly found in food processing and manufacture. The objective of this study was to understand the effect of shear stress on L. *monocytogenes* in single and dual-species (with *P. fluorescens*) biofilm formed in a continuous turbulent flow system. In the single-species biofilm, *L. monocytogenes* was able to form a biofilm under the turbulent flow with cell concentration reaching 5.1 log CFU/cm^2 after 48 h, where filamentous cells (27.7 μm in length) were observed. In contrast, there were no visible filaments in the dual-species biofilm, and L. *monocytogenes* cell concentration was significantly higher ($p < 0.001$) at 8.7 log CFU/cm^2. The cells harvested from single-species L. *monocytogenes* biofilm formed under turbulent flow showed significantly ($p < 0.001$) lower motility and higher adhesion compared with cells harvested from planktonic and static conditions. Gene expression analysis showed significant ($p < 0.001$) downregulation of *motB* (motility), *sigB* (stress), and cell division (*ftsX* and *ftsW*), and upregulation of *mpl* (adhesion) and *rodA* (rod shape), indicating L. *monocytogenes* adaptation to shear stress. This study provides fundamental information on the multi-species biofilm formation by L. *monocytogenes* under stress.

1. Introduction

Listeria monocytogenes are rod-shaped, non-spore-forming, gram-positive bacteria, and an important foodborne pathogens that commonly cause outbreaks in dairy products (raw milk, ice cream, cheese), meat products (deli meat), fresh fruits (peaches, cantaloupes) (Redding et al., 2024), and vegetables (enoki mushrooms, leafy greens) (Wiktorczyk-Kapischke et al., 2023). They can persist in the food industry, often showing enhanced resistance to adverse conditions such as low temperature (−1.5 °C), low nutrients, acidity (pH: 3.3–4.2), salinity (10 %), and chemicals (lethal/sublethal) (Melian et al., 2022; Papaioannou et al., 2018; Wiktorczyk-Kapischke et al., 2021). These stress adaptations can be the result of quorum sensing between the bacteria (Zhu et al., 2017), upregulation of stress genes, which are regulated by the sigma factor σ^B (Guerreiro et al., 2020), resulting in the expression of virulence genes, and changes in phenotypic traits (Wiktorczyk-Kapischke et al., 2023).

Homeoviscous adaptation for low-temperature survival (Miladi et al., 2013), rod to coccoid shape under nutrient stress (Gao & Liu, 2014), and rod to elongated chains under saline stress (Giotis et al., 2007; Shah & Bergholz, 2020) are some of the examples of stress adaptation by L. *monocytogenes*. The filamentation of planktonic L. *monocytogenes* under saline stress has been correlated with the expression of genes related to the upregulation of the min C gene (inhibits septa formation) (Kale et al., 2017), downregulation of *lmo2506* (cell division), *lmo2552* (cell wall synthesis), and *lmo1376* (NADPH production) (Liu, Miller, et al., 2014). The phenotypic change includes the elongation of cells longer than 4 μm as compared to the 'normal' cell length of L. *monocytogenes*, which is 1–2 μm (Yamaki et al., 2021). *L. monocytogenes* isolated from conditions of shear stress have higher adhesion to abiotic surfaces (Mendez et al., 2020) and enhanced resistance to removal through shear stress (Szlavik et al., 2012; Vázquez-Boland et al., 2001). The formation of filamentous cells under stress results in the underestimation of the L. *monocytogenes* cell count (Bereksi et al., 2002; Jones et al., 2013). Once the stress factor is removed, rapid proliferation of L. *monocytogenes* is observed, contributing to foodborne outbreaks (Yamaki et al., 2021).

The adaptation designed for one stress factor that aids bacteria in surviving multiple stress factors is known as cross-tolerance. For example, adapting to cold stress aids in the adhesion of the bacteria to

* Corresponding author.
E-mail address: kpant@massey.ac.nz (K. Pant).

https://doi.org/10.1016/j.foodres.2025.117190
Received 29 May 2025; Received in revised form 28 July 2025; Accepted 30 July 2025
Available online 5 August 2025

stainless steel surfaces and resistance to quaternary ammonium compound sanitizer (Miladi et al., 2013). Similarly, the stress resistance obtained in low-temperature growth improves the cross-tolerance to osmolarity stress (Schmid et al., 2009). The stress-tolerance of L. *monocytogenes* has been positively correlated with the predominance of L. *monocytogenes* in polymicrobial communities in food processing environments (FPEs) (Wang et al., 2023). This synergistic interaction of L. *monocytogenes* with the background microbiota on FPEs enhances biofilm formation and resistance against sanitizers (Gu et al., 2024; Ibusquiza et al., 2012; Puga et al., 2018). Pang and Yuk (2019) observed higher resistance of L. *monocytogenes* against environmental stresses when L. *monocytogenes* was incorporated into *P. fluorescens* preformed biofilm, indicating the importance of multispecies interactions in biofilm eradication. This can result from the utilization of extracellular matrix components such as exopolysaccharide (EPS) and metabolites produced by the background microbiota, such as *P. fluorescens* (Flemming et al., 2016; Puga et al., 2018). *P. fluorescens* is a major spoilage microorganism frequently isolated from dairy surfaces (Maggio et al., 2021) and has been studied extensively for its role in the synergistic multispecies biofilm (Puga et al., 2018; Zhou et al., 2024). *P. fluorescens* has been reported to produce higher proteolytic enzymes in mixed-species biofilm (Teh et al., 2014) harbour weak biofilm formers (Puga et al., 2015) and show enhanced protection of the overall biofilm from desiccation and disinfection (Pang & Yuk, 2019).

One important factor is understanding the effect of shear stress on biofilm formation of pathogens such as L. *monocytogenes* in single and multi-species communities. So far, studies on the stress response of L. *monocytogenes* are limited to pH, saline, bile, and nutrients and are focused on planktonic cells, disregarding the most common form of bacteria in nature, the biofilm. In the food processing industries, there are unit operations such as fresh-cut in the minimal processing vegetables (MPV) sector (Cunault et al., 2015), storage (transport) tanks in the dairy sector (Alabdullatif, 2024), spray drying systems (Al-Sharify et al., 2025), and flow through stainless-steel tubes (Perni et al., 2006), where the impact of hydrodynamic conditions can be observed (Szlavik et al., 2012). The biofilm formation, composition, structure, and finally the difficulty of removal from the surface are dependent on many factors such as hydrodynamic conditions, properties of the material, nutrient abundance, and temperature (Simões et al., 2022). Flow conditions and nutrient supply to the bacteria are recognized as important variables in biofilm development (Prabhukhot, Eggleton, Kim, & Patel, 2024; Simões et al., 2022; Vázquez-Boland et al., 2001).

Previous research has also stated the difficulty in the removal of biofilm formed under flow compared to biofilms formed under static conditions (Vázquez-Boland et al., 2001). This research aims to understand the effects of shear stress on the biofilm formation of L. *monocytogenes* and the cross-adaptation it develops because of shear stress. The morphology of L. *monocytogenes* under turbulent flow in the presence *P. fluorescens* on industrially relevant stainless-steel surfaces was also studied.

2. Materials and methods

2.1. Bacterial strains and culture media used

Pseudomonas fluorescens 2614 (P1) (dairy isolate) collected in March 2019 with access code P1DZ and *Listeria monocytogenes* H1 (environment-soil isolate) collected in October 1997 with access code H1KP were used for biofilm formation, which are from a previously established culture collection (Food Microbiology Lab, School of Natural Sciences and Food Technology, Massey University, Palmerston North). The bacteria stored in glycerol stock

(−80 °C) were inoculated into tryptone soy broth (TSB) (Difco™, Becton, Dickinson and Company, USA) and incubated at 30 °C for 20 h. The bacteria were centrifuged (Sigma® 6–16, John Morris Scientific Ltd., New Zealand) at 3000*g* for 20 min, and the supernatant was discarded. The cell pellets were resuspended in saline solution (0.85 %) and centrifuged for another 20 min. Finally, the saline solution was discarded, and the cell pellets were redissolved into fresh saline solution. The cell concentration was adjusted to 8 log CFU/mL using a graph of $O{\cdot}D_{600}$ nm vs. cell concentration (log CFU/mL) ($R^2 = 0.97$) for individual bacteria. For dual species, each bacterium was adjusted to this cell concentration and added in 1:1 concentration during inoculation, keeping the ratio of media to cells the same as in single species.

2.2. Biofilm formation in static and turbulent conditions

Stainless steel coupons (type 316, 2B finish, 2.4 cm^2) (Advanced Sheetmetals Ltd., Palmerston North) were used for biofilm formation in static conditions (Skowron et al., 2019). The coupons were passivated (50 % nitric acid at 70 °C for 30 min) to generate a chromium oxide coat, followed by washing, drying, and autoclaving (121 °C, 15 mins). The sterile coupons were added to 48-well plates (Costar®, Falcon, USA) containing 10 % TSB with a final cell concentration of L. *monocytogenes* adjusted to 6 log CFU/mL. The plates were incubated at 30 °C for 24 h for further analysis of static biofilm.

The Centre for Disease Control (CDC) bioreactor (Biosurface Technologies Corporation, USA) was used for single and multispecies biofilm formation under shear stress (Prabhukhot, Eggleton, Vinyard, & Patel, 2024). Each bioreactor consisted of 8 rods (3 coupons in each rod), and the bioreactor was connected to the sterile media influent and waste media effluent. Bacteria in single and dual-species (1:1) were added to 300 mL of sterile media in the bioreactor to fix the starting cell concentration at 6 log CFU/mL. The sterile media (10 % TSB) was pumped at 5 mL/min according to the bacteria's doubling time. The CDC bioreactor was run for seven days under continuous flow, at 30 °C and 250 rpm using a heating magnetic stir plate (VWR International, U.S.A). Depending on the experiments, rods were taken out at appropriate time intervals for cell concentration analysis, microscopic observations, and genetic analysis.

For the dynamics of the biofilm formation in single and dual species, one rod (three coupons) was taken out of the bioreactor every 24 h for 7 days. The blank rod replaced the coupon rod to maintain the flow. The coupons were saline washed to remove planktonic cells, and the cell concentration in the biofilm was estimated using bead beating assay (3 g glass beads (diameter − 5 mm, Sigma-Aldrich, Germany) in 5 mL saline solution, mixed by vortex for 5 min) and plated in selective agar. *Pseudomonas* Isolation agar (Difco™, USA) was used to enumerate *Pseudomonas*, and Modified Oxford agar (HiMedia, USA) was used to enumerate *Listeria* from the dual species samples. A similar method was repeated for single-species biofilm as well, where the coupons were saline washed, bead-beaten, and plated on tryptone soy agar (TSA). The bioreactors were run for 2 biological replicates for each sample, and each biological replicate consisted of 3 technical replicates.

2.3. Reynolds number for turbulent flow

The Reynolds number of the fluid flowing through the bioreactor was determined to estimate the turbulence in the media ($Re < 2100$-laminar, $2100 < Re < 4000$-transient, $Re > 4000$-turbulent) (Prabhukhot, Eggleton, Kim, & Patel, 2024; Prabhukhot, Eggleton, Vinyard, & Patel, 2024). The Reynolds number was calculated according to the modified equation for the tangential velocity of media in the agitated vessel.

$$Re = \frac{v^{*}Dh}{\mu} \tag{1}$$

where *Re* is the Reynold number, v is the hydrodynamic velocity, Dh is the diameter of the annulus given by 2 (R_o-R_i), R_o is the outer radius measured from the impeller center to the inner coupon surface, R_i is the inner radius measured from the impeller center to the outer edge of the impeller, and μ is the kinematic viscosity (1.0023E-06 m^2/s).

2.4. Cross-adaptation: cells from planktonic, static, and turbulent flow

The cells were harvested from the biofilm at 48 h incubation time, formed in turbulent flow and static conditions using glass-bead beating in saline solution (5 min), sonication (5 min), and followed by centrifugation (5 min, 12,000 g) (Niboucha et al., 2022). The cells from the planktonic culture were harvested through centrifugation (5 min, 12,000 g). The supernatant was discarded for both cases, and the cells were washed in saline solution and centrifuged again for 5 min at 12,000 g. The final cell pellet was dissolved in saline solution, and the cell concentration was fixed at 6 log CFU/mL before the following analysis was carried out with the harvested cells.

2.4.1. Motility

The motility of the cells harvested from planktonic, static, and turbulent flow was observed through swimming agar according to (Li et al., 2018) with modifications. A volume of 2 μL inoculum (6 log CFU/mL) was stabbed into 0.3 % agar in tryptone soy broth (TSB) agar plates, and the diameter of the growth at 30 °C after 24 h was measured using a vernier calliper.

2.4.2. Adhesion to stainless-steel surface

The variation in the adhesion of L. *monocytogenes* cells with filamentation (shear-stressed cells) and without filamentation (static and planktonic) was observed using stainless steel coupons (Wang et al., 2022). A volume of 100 μL of harvested cells (6 log CFU/mL) was inoculated into 10 % TSB in a 48-well plate and incubated for 5 min at 30 °C to investigate the initial attachment of the bacteria harvested from different growth conditions on the stainless steel surface (Rodriguez et al., 2008). After the incubation, the coupons were removed, washed in saline solution, and cells adhered to the stainless-steel surface were enumerated using the glass bead beating method (3 g glass beads in 5 mL saline solution, mixed by vortex for 5 min) and enumerated on TSA using a spread plate method. The relative adhesion of the cells was calculated by dividing the log of the attached bacteria by the log of bacteria in the inoculum (Chae & Schraft, 2000).

2.4.3. Biofilm-forming ability of harvested cells

The cells harvested from planktonic culture, static biofilm, and turbulent flow biofilms were used as inoculum (adjusted to 6 log CFU/mL) to form biofilm on the stainless-steel coupons (type 316, 2B finish, 2.4 cm^2) at 30 °C for 24 h in 10 % TSB under static conditions. The cells in the biofilm formed were quantified through the glass bead beating method and enumeration on TSA plates as described above (Section 2.4.2).

2.5. Epifluorescence- morphology of the cells

Acridine orange stain (10 g/L) (BDH, England) was used to visualize the cells as a biofilm after 48 h incubation on stainless-steel coupons in the CDC bioreactor and static coupon surfaces and planktonic cells. The coupons were removed from the bioreactor with mono-species L. *monocytogenes* biofilm at 48 h and washed with saline solution to remove planktonic cells. The washed and air-dried coupons were dipped in acridine orange staining solution for 5 min and washed with saline solution before air-drying and visualization using an epifluorescence microscope (Nikon eclipse Ni, USA) with TRITC (excitation filter 485/20 nm and emission filter 500–538 nm) and NIS-elements D software. Five images were captured from each coupon. Three technical replicates were acquired from each biological replicate. Two biological replicates were used for microscopic analysis. The length and width of at least 20 cells were measured for each replicate, and the results were presented as mean ± standard deviation.

2.6. Fluorescence in situ hybridization (FISH) and confocal microscopy

Dual-species biofilm samples were collected from the bioreactor at 48 h, stained with a fluorescent probe (Custom Taqman®, Life Technologies, CA, USA) (Kocot & Olszewska, 2020) and counterstained with 4′,6-diamino-2-phenylindole (DAPI) (Invitrogen, Thermo Fisher Scientific, USA) and visualised using confocal microscopy (Nikon D-eclipse C1, Japan). Coupons were washed with PBS before fixing in 4 % paraformaldehyde (BDH Limited, Poole, England) for 15 min at room temperature. The fixed coupons were treated with lysozyme (1 mg/mL) (Sigma-Aldrich, Belgium) at 37 °C for 10 min. The treated coupons were washed with PBS and air-dried before staining with the fluorescent probe at 46 °C for 2 h. The coupons were then dipped in wash buffer at 48 °C for 15 min before counterstaining with DAPI (1 mg/mL) and incubation in the dark at room temperature for 10 min. The coupons were finally washed with PBS and air dried before visualization of the cells using blue channels for DAPI and red channels for the FISH stain. A 60× water immersion lens was used to observe the images. The images were acquired and overlayed using EZ-C1 software (Gold version 3.80 build 860).

2.7. Relative gene expression

Based on the observations made above (Section 2.4), the variation in the expression of the genes relating to the motility of the cells (*motB*), stress (*sigB*), biofilm formation and adhesion (*mpl*), rod shape (*rodA*), and cell division (*ftsW* and *ftsX*) was observed for samples collected from static and turbulent flow and compared to planktonic cells (Gao et al., 2024). 16S and rpoB genes were reference genes for this experiment (Table 1).

The cells from the static and turbulent flow biofilms were collected using ice-cold, acid-treated glass beads (Sigma, Germany) and phosphate buffer saline (PBS) mixed by vortex for 5 min, followed by sonication for 5 min. The sonicated solution was centrifuged, and the pellets were collected for RNA extraction. The planktonic samples were centrifuged after 24 h incubation (30 °C), and cell pellets were collected for further analysis. The RNA was extracted and purified from the planktonic, static, and shear-stressed samples using NucleoSpin® RNA Plus (Macherey-Nagel, Germany). The integrity of the extracted RNA was analysed using a Nanodrop (Jenway, Bibby Scientific Ltd., UK), and

Table 1
Primer sequences used for gene expression analysis of *Listeria monocytogenes*.

Gene	Primer	Sequence	References
16S-reference gene	Forward	ACATCCTTTGACCACTCTGGA	(Gao et al., 2024)
	Reverse	CAACATCTCACGACACGAGC	
rpoB	Forward	CGTCGTCTTCGTTCTGTTGG	(Gao et al., 2024)
	Reverse	GTTCACGAACCACACGTTCC	
motB	Forward	TGCAAAAAAATTCGAACAAATGG	(Gao et al., 2024)
	Reverse	CTGCCGCGCCTTCCT	
sigB	Forward	AAAGAAACGGGTGAACTACTCGAT	(Gao et al., 2024)
	Reverse	CAACGCCTCTCGAAGTTTTTTAA	
mpl	Forward	CGGTTATCCAGTATTCGGCG	(Gao et al., 2024)
	Reverse	TTCCTCTGTGAGTGGAAGCG	
rodA	Forward	CTTCCGCTTGGTCTTGTAGC	(Liu, Basu, et al., 2014)
	Reverse	CAATGAGCGCAATCGAACTA	
ftsW	Forward	GGGATCGCTAGTCTGATTGC	(Liu, Miller, et al., 2014)
	Reverse	TACCAAGCATCATCGACAGC	
ftsX	Forward	AATGGTTGGATGACCTTTGC	(Liu, Miller, et al., 2014)
	Reverse	CGTTGCAAGCTTGTTCATGT	

the A260/A280nm ratio of 1.9 and above was selected for RT-qPCR (LightCycler® 480, Roche Diagnostics, Switzerland). A total volume of 20 μL consisted of SYBR@Green mastermix, primers (forward and reverse), DNA template, and PCR-grade water, and the RT-qPCR conditions were set according to Luna® Universal One-step RT-qPCR Kit (New England Biolabs, Ipswich, MA). The fold change was analysed using the $2^{-\Delta\Delta ct}$ for the target genes (Livak & Schmittgen, 2001) with reference gene (16S) as internal control (Table 1). The non-template control (NTC) was tested for each set of primers.

2.8. Statistical analysis

The length of the cells in planktonic, static biofilm, and turbulent biofilm samples was measured using ImageJ (ImageJ 1.54 g, National Institute of Health, USA) from the images obtained from the epifluorescence microscope. The significant differences ($p < 0.05$) between the samples were analysed using one-way ANOVA (IBM SPSS Statistics 29) and post-hoc analysis using Tukey's test, and results were represented as mean ± S.D. The relationship between the length of the cells with motility, adhesion to the stainless-steel coupons, and biofilm formation at 24 h was analysed using Pearson's correlation analysis (IBM SPSS Statistics 29).

3. Results

3.1. Biofilm formation under turbulent flow

The Reynolds number of the flowing media in the bioreactor was higher than 4000, confirming turbulent flow in the CDC bioreactor. In the single-species biofilm, the cell concentration of *P. fluorescens* at 24 h was 6.3 log CFU/cm^2, which gradually increased to 7.8 log CFU/cm^2 over the next 6 days of incubation. In the single-species, *L. monocytogenes* showed a gradual increase in cell concentration from 4.7 log CFU/cm^2 (day 1) to 6.3 log CFU/cm^2 (day 7)
(Fig. 1).

The biofilm formation of *P. fluorescens* was similar in dual species (with L. *monocytogenes*), with cell concentrations ranging from 6.4 to 7.5 log CFU/cm^2 during a 7-day incubation period (Fig. 1). Significantly higher growth ($p < 0.05$) of L. *monocytogenes* was observed in dual-species, compared to single-species biofilm (Fig. 1). While the cell concentration of *Listeria* in 24 h biofilm was comparable in single (4.7 log CFU/cm^2) and dual-species (5 log CFU/cm^2), a significant increase ($p < 0.005$) was observed at 48 h where the cell concentration of *Listeria* was significantly higher ($p < 0.05$) in dual species (8.7 log CFU/cm^2) biofilm as compared to its single species counterpart (5.1 log CFU/cm^2). After this initial rise over 48 h in dual species, the cell concentration of *Listeria* remained consistent over 7 days (8.7–9 log CFU/cm^2)

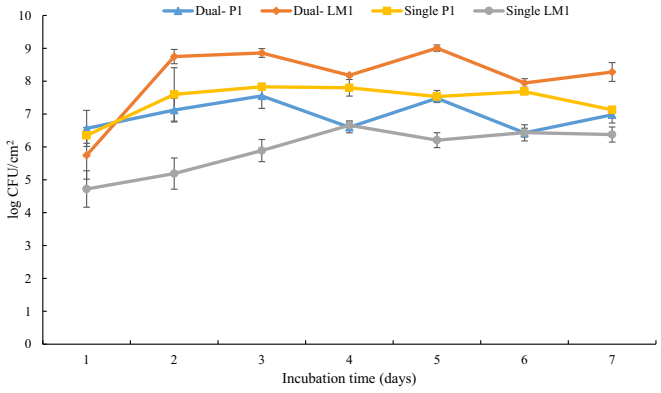

Fig. 1. Cell concentration of *P. fluorescens* (P1) and L. *monocytogenes* (LM1) in single- and dual-species biofilms formed under turbulent flow in the CDC bioreactor during 7-day incubation at 30 °C.

(Fig. 1).

3.2. Spatial arrangement and morphology of the cells

A 'knitted' or 'web' structure (Fig. 2.A) was observed in 72 h *L. monocytogenes* single species biofilm formed under turbulent flow, which, under higher magnification, was observed to be overlapping of filaments (Fig. 2.B). While the filament structure was absent in dual-species biofilm formed with *P. fluorescens* under turbulent flow, a 'web' structure was observed (Fig. 3).

The average length of the 'normal' *L. monocytogenes* cells in planktonic and static biofilm was 1.3 ± 0.2 μm and 1.4 ± 0.2 μm, respectively ($p > 0.05$). In comparison, the length of the shear-stressed cells observed in the bioreactor reached 27.7 ± 6.2 μm (refer to Fig. 4. C for an example), which increased in length up to 72 h of incubation. The length of the filaments reached as high as 52.3 ± 1.1 μm under the same conditions. In dual-species biofilm formed by *P. fluorescens* and L. *monocytogenes*, filaments were completely absent, with the mean cell length of 1.6 ± 0.3 μm under flow conditions, indicating no morphological changes of L. *monocytogenes* in the presence of the second bacterium (*P. fluorescens*) (Fig. 3). Overall, the bacterial width was unaffected ($p > 0.05$) in all growth conditions in single-species biofilm, ranging 0.48 ± 0.06 μm, 0.46 ± 0.05 μm, and 0.46 ± 0.04 μm for planktonic, static, and

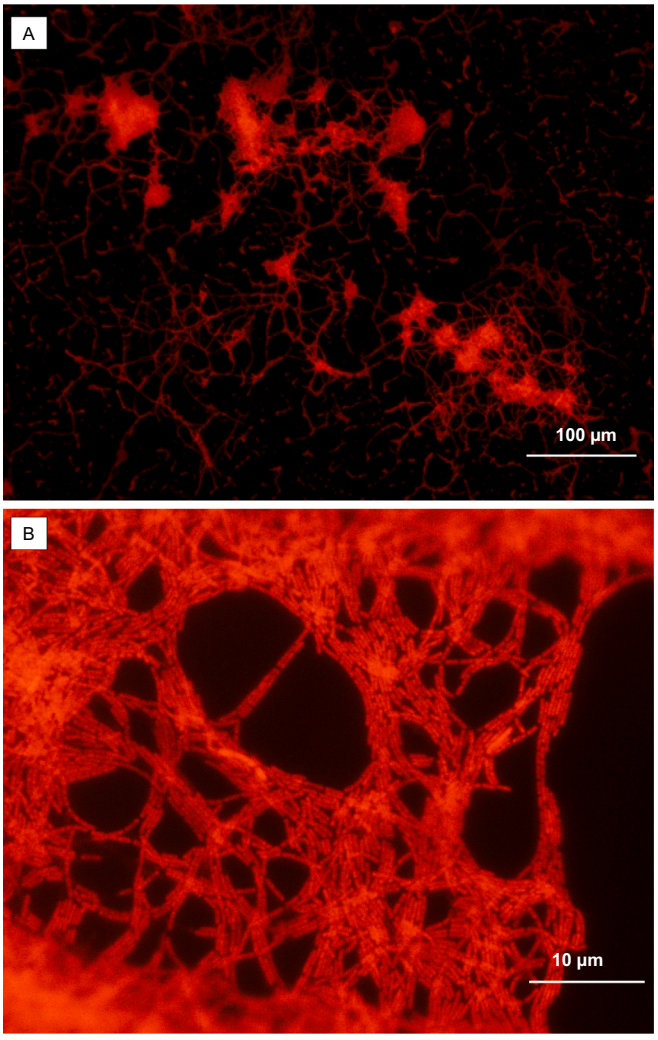

Fig. 2. Knitted structure of L. *monocytogenes* in single-species biofilm formed under turbulent flow (CDC bioreactor) at 30 °C for 72 h, observed with epi-fluorescence microscopy and acridine orange staining under two different magnifications: A) 400× and B) 1000×.

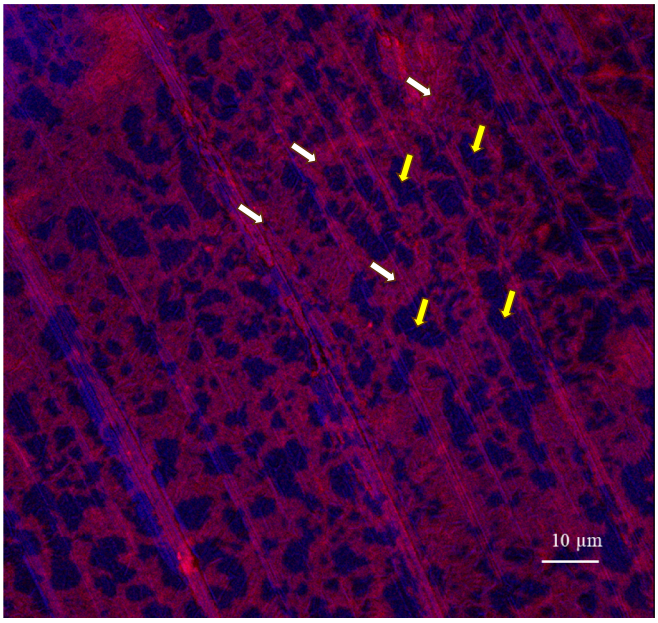

Fig. 3. Confocal microscopy image (60× immersion lens) showing a web-like structure of L. *monocytogenes* (red-cyanine red probe) on *P. fluorescens* (blue-DAPI) layer, observed for a dual-species biofilm formed in a CDC bioreactor at 30 °C. Note: the yellow arrows indicate *P. fluorescens* cells (blue) and the white arrows indicate L. *monocytogenes* cells (red). (For interpretation of the references to colour in this figure legend, the reader is referred to the web version of this article.)

turbulent flow, respectively. A similar observation ($p > 0.05$) of cell width (0.45 ± 0.07 µm) was made for L. *monocytogenes* cells in a dual-species biofilm with *P. fluorescens*.

3.3. Cross-adaptation and correlation

The motility of the cells harvested from biofilm formed under turbulent flow was significantly lower ($p < 0.05$) (3.4 ± 0.9 mm) than those harvested from static biofilm (15.3 ± 1.6 mm) and planktonic conditions (21 ± 5.6 mm), observed as the diameter of the growth in 0.3 % TSB agar (Fig. 5.B). The motility negatively correlated (Table 2) with the adhesion of the bacteria (5 min) on stainless steel surfaces in 10 % TSB. The highest relative adhesion ($p < 0.05$) (5 mins) was observed for cells from turbulent flow (66.4 ± 7.6 %) compared to cells harvested from planktonic (51.8 ± 4.3 %) and static systems (51.9 ± 6.7 %) (Fig. 5.A). The higher relative adhesion of cells from turbulent flow resulted in lower cell numbers in biofilms ($p < 0.05$) in the turbulent flow (6.7 ± 0.07 log CFU/cm^2) biofilms compared to static (7.2 ± 0.1 log CFU/cm^2) and planktonic systems (7.0 ± 0.1 log CFU/cm^2) (Fig. 5.C).

Overall, the length of the cells had a positive impact on adhesion and a negative correlation with motility and biofilm formation. Meanwhile, bacteria with higher motility showed reduced adhesion, but this had a weak correlation with biofilm. The bacteria's adhesion showed a weak negative correlation with biofilm, but the correlation was not statistically significant (Table 2).

3.4. Relative gene expression

The cells from the turbulent flow system showed significant ($p < 0.001$) downregulation of motility gene (*motB*), stress gene (*sigB*), and cell division genes (*ftsW* and *ftsX*), whereas adhesion gene (*mpl*) and rod shape determining gene (*rodA*) were found to be significantly ($p < 0.001$) upregulated, relative to cells harvested from the planktonic and static system (Fig. 6).

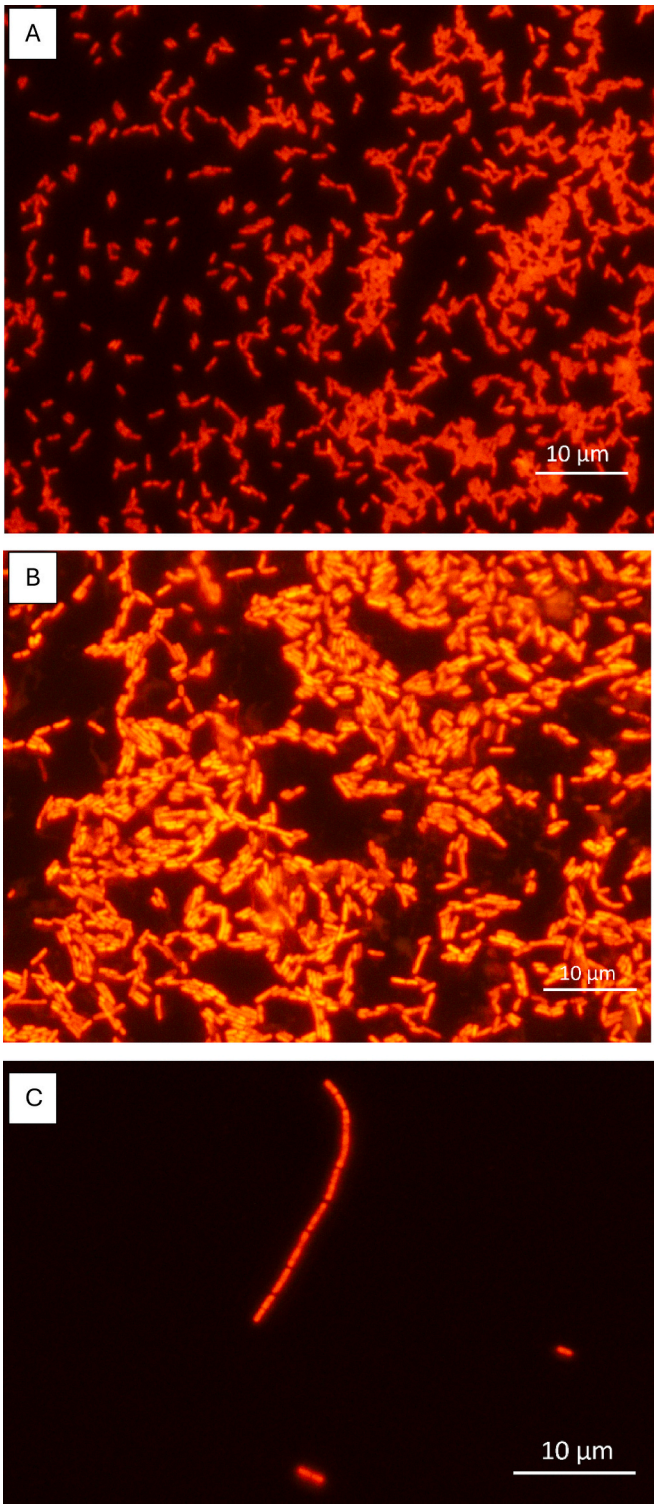

Fig. 4. *L. monocytogenes* cells morphology under different conditions. A) Cells in 24 h planktonic culture, B) Cells in 48 h static biofilm, C) Cells in 48 h CDC bioreactor, all incubated at 30 °C.

4. Discussion

In this study, the cell concentration of L. *monocytogenes* improved significantly ($p < 0.05$) in dual-species biofilm compared to its single-species counterpart under turbulent flow during a 7-day incubation period (Fig. 1). *L. monocytogenes* is a relatively poor biofilm former, and its inability to form biofilm under shear stress has been noted before

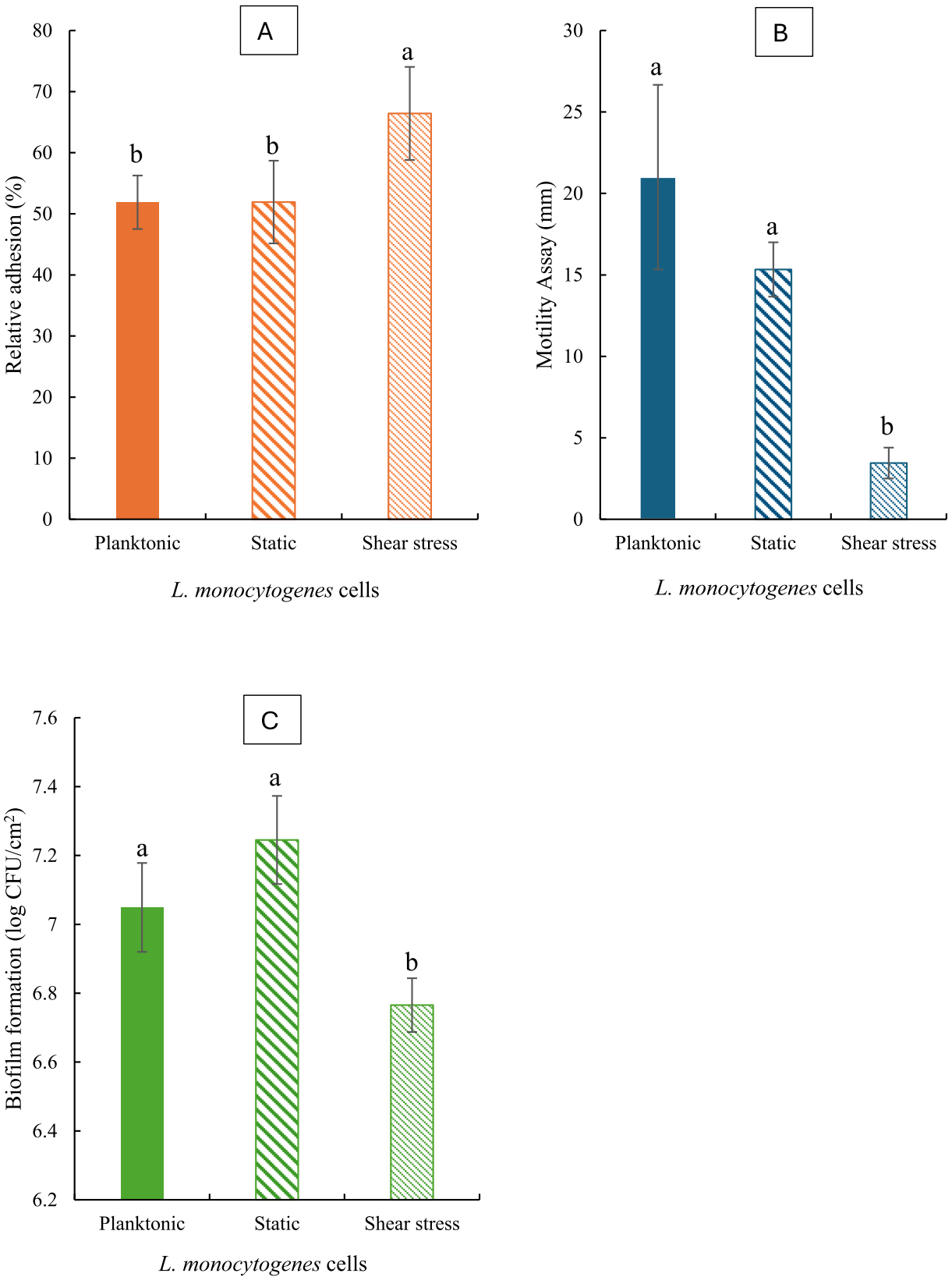

Fig. 5. Observations made for planktonic, static, and shear-stressed cells at 30 °C, A) Relative adhesion (%), B) Motility (0.3 % agar), C) Cell count in biofilm (24 h).

(Fagerlund et al., 2021). Under turbulent flow, the presence of higher exopolysaccharide-producing bacteria (*Pseudomonas*) was found to be more impactful in increasing the biofilm formation of L. *monocytogenes* than the hydrophobicity, surface charge, or the motility of L. *monocytogenes* (Sasahara & Zottola, 1993). A similar observation was made for *Pseudomonas* and L. *monocytogenes* dual-species biofilm formed on the glass coverslips under flow, where improved cell concentration was observed for L. *monocytogenes* in dual-species compared to its mono-

Table 2
Correlation between cell length, motility, adhesion, and biofilm formation (24 h) observed with Pearson's coefficient.

	Length	Motility	Adhesion	Biofilm
Length	1	−0.880**	0.869**	−0.758*
Motility	−0.880**	1	−0.846**	0.49
Adhesion	0.869**	−0.846**	1	−0.415
Biofilm	−0.758*	0.49	−0.415	1

** Correlation is significant at the 0.01 level; * Correlation is significant at the 0.05 level.

species counterpart (Puga et al., 2018). An observation of the spatial arrangement of the bacteria via confocal microscopy showed that L. *monocytogenes* cells embed themselves at the bottom of the biofilm, under the protective layer of *P. fluorescens*, protecting themselves against the shear forces (Puga et al., 2018). In another study of dual-species biofilm formed by L. *monocytogenes* and *P. fragi* under a flow system, the L. *monocytogenes* cells' mobility was limited to a localised surface area and appeared to be trapped between the *P. fragi* cells and the EPS matrix, providing protection against the flow (Sasahara & Zottola, 1993). Under a different growth condition (static), the cell concentration of *L. monocytogenes* decreased (6.7 log CFU/cm^2) in dual-species biofilm formed with *P. fluorescens* compared to its single-species biofilm (7.21 log CFU/cm^2), while *P. fluorescens* maintained its cell concentrations (7.5–7.8 log CFU/cm^2), indicating the importance of flow on the behaviour of bacteria in multispecies setups (Pang & Yuk, 2019).

The present study observed chain-like filamentation in L. *monocytogenes* cells of the single-species biofilm formed under turbulent flow (Figs. 2 and 4.C), indicating that this adaptation results from high hydrodynamic shear stress. A similar observation was made for *L. innocua* cells under shear stress, where elongation of specific cells was noted for several cells adhered to the stainless-steel surface (Perni et al., 2006). In L. *monocytogenes*, conditional filamentation of bacteria has been attributed to two major conditions: environmental stress and starvation (Karasz, Weaver, Buckley, & Wilhelm, 2022). These conditions trigger DNA lesions, and filamentation has been reported as a response to repair these lesions (Jones et al., 2013), resulting in inadequate cell separation and the visualization of filament structures. The average length of L. *monocytogenes* conditioned with 10 % NaCl for 3 days was found to be 6.5 ± 3.3 μm (Yamaki et al., 2021), indicating adaptation to salinity stress under sublethal conditions. The plating of the filaments may not necessarily separate the cells during enumeration, leading to an underestimation of the total cell count (Giotis et al., 2007). Once filamentation is triggered, returning to the 'normal' state depends on the type of stress that caused filamentation. For example, alkali-stressed *Listeria* cells required three hours to revert to normal-sized cells when incubated in fresh media with neutral pH conditions (Giotis et al., 2007), whereas CO_2-stressed *Listeria* cells took longer (2–4 days) to revert to their original morphology (Jydegaard-Axelsen, Aaes-Jørgensen, Koch, Jensen, & Knøchel, 2005). In addition to the filamentous structure, in the present study, a knitted pattern was observed in 48-h biofilms formed by L. *monocytogenes* in single-species (Fig. 2) and in dual-species (Fig. 3). A similar observation of a 'web-like' structure was noted for L. *monocytogenes* formed under flow and nutrient stress in a microfluidic system (1/10 BHI) (Cherifi, Jacques, Quessy, & Fravalo, 2017) or 'knitted' structure in flow cell chambers (1 % TSB) (Rieu et al., 2008). This pattern changed under the lack of nutrient stress (full-strength BHI), revealing layered bacterial structures (Cherifi et al., 2017).

In a dual-species biofilm with *P. fluorescens*, no filamentous structure was observed (Fig. 3) and was accompanied by significantly ($p < 0.001$) higher cell concentrations of L. *monocytogenes* (Fig. 1). In the case of layering, the upper layer consists of metabolically active cells, while the lower layer contains metabolically inactive cells, as observed in *Lactobacillus lactis* biofilm (Habimana et al., 2009). This phenomenon has been explained in terms of nutrient access to the top of the biofilm compared to the bottom (Habimana et al., 2011). The predominant nature of other bacteria over L. *monocytogenes* has been associated with

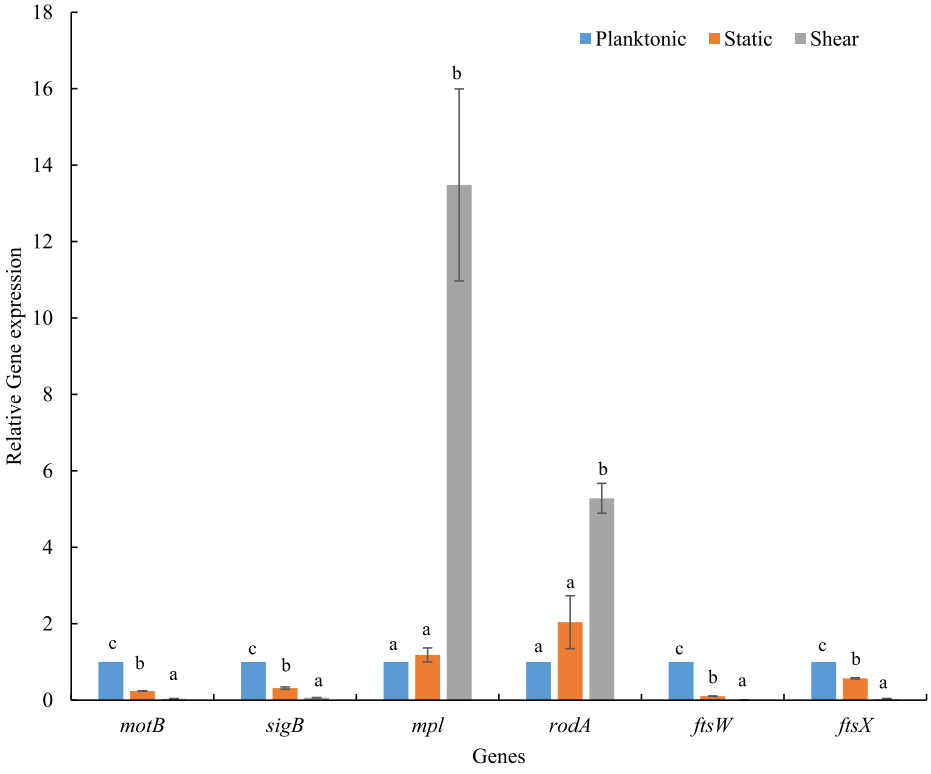

Fig. 6. The relative gene expression (fold change) of cells from the planktonic system, static biofilm, and biofilm formed under turbulent flow. (Different letters represent significant differences between each bar in a triplicate set – ie. For each gene).

differences in growth rates, which result in the smothering of L. *monocytogenes* into the lower layers of the biofilm, leading to competitive inhibition (Habimana et al., 2011). However, in the present study, in the continuous system with *P. fluorescens* and L. *monocytogenes* although *P. fluorescens* predominated, no competitive inhibition was observed for either bacterium over 7 days (Fig. 1).

While adhesion is one of the first steps for biofilm establishment, this study found a weak correlation between adhesion (5 min) and biofilm formation (24 h) in terms of cell concentration (Table 2). A negative correlation was observed between motility and adhesion, resulting in higher adhesion of *Listeria* in filament forms on the stainless-steel surface. In a similar study, *L. monocytogenes* strains with low or no motility were found to form a higher biofilm at 37 °C (Fan et al., 2020). Rapid adhesion provides the bacteria an opportunity to adhere firmly to the surface and form stronger biofilms before the cleaning and disinfection (Wang et al., 2022). In contrast, the adhesion period of 30 min on polystyrene surfaces showed no linear correlation between adherence and motility of L. *monocytogenes* on polystyrene surfaces (microtiter plate) (Takahashi et al., 2010), indicating the importance of the duration of adherence. The variation could also be the result of surface hydrophobicity (plastic surfaces). The lack of correlation between L. *monocytogenes* adherence and biofilm formation has been noted before on glass surfaces (3 h) (Chae & Schraft, 2000).

A significant downregulation ($p < 0.05$) of the *motB* gene was observed in cells harvested from biofilm under static and flow conditions (Fig. 6). The motility of the cells is associated with the regulation of the *motB* gene, which regulates the flagella rotation, expressing the swimming and swarming abilities of the bacteria (Fan et al., 2020) and also regulates chemotaxis protein. The downregulation of motility genes results in the paralysis of flagella, resulting in cells with decreased swimming and swarming properties of the bacteria (Jiang et al., 2025). In the present study, motility was positively associated with adhesion (5 mins) but did not correlate with biofilm formation (24 h) (Fig. 5). Depending on the L. *monocytogenes* strain, media, and growth temperature, a conflicting relationship between motility and biofilm formation can be found in the literature. A positive impact of motility and biofilm formation has been noted for L. *monocytogenes* (Fan et al., 2020; Gao et al., 2024). In contrast, Dong et al. (2022) observed no impact of motility on the biofilm formation for L. *monocytogenes*. The significant upregulation of the *mpl* gene during biofilm formation on stainless steel surfaces has been noted previously, indicating its importance in biofilm formation (Gao et al., 2024). The upregulation of the *mpl* gene in the present study, corresponded with the significantly higher adhesion ($p < 0.05$) to the stainless-steel surface for the shear-stressed cells (Fig. 5.B).

A significant downregulation of the stress-regulating gene (*sigB*) was observed for cells collected from shear-stressed conditions compared to cells collected from planktonic conditions (Fig. 6). The stress factor gene, *sigB,* controls the general stress response (GSR) (Santos et al., 2019) and is assumed to trigger resistance to environmental and antibiotic stress in L. *monocytogenes,* resulting in cross-tolerance (Poimenidou et al., 2023). Upregulation of the *sigB* genes was observed in the presence of flow (van der Veen & Abee, 2010) and NaCl (2 % and 5 %). However, reports also suggest that the stressful conditions do not necessarily result in upregulation of *sigB*, but vary depending on the L. *monocytogenes* strains, growth stages, and conditions (van der Veen & Abee, 2010). Under cold stress, higher expression of stress genes was observed for the biofilm during the mature stage (Santos et al., 2019), in contrast to the study by (Utratna et al., 2014), where the expression was highest in the early stages of biofilm formation. In the present study, the application of hydrodynamic stress in the continuous system corresponds to the constant influx of fresh media into the bioreactor and removal of waste media from the bioreactor, which could negate the nutritional stress that planktonic cells and static cells encounter in a closed system. Additionally, the *sigB* gene was found to be significantly downregulated in the combined treatment of sodium hypochlorite + peroxyacetic acid and hydrogen peroxide + peroxyacetic acid (Byun et al., 2024), and Quercetin (0.2 mM and 0.8 mM) treatment (Vazquez-Armenta et al., 2020), indicating the role of suppression of *sigB* genes in reduced biofilm formation.

The Fts and rodA proteins belong to the family of SEDS (shape, elongation, division, sporulation) proteins (Rismondo et al., 2019). In the present study, significant downregulation of genes (*ftsW* and *ftsX*) and upregulation of gene *rodA* was observed (Fig. 6). This correlated with the microscopic observations of biofilm formed under turbulent flow, which showed the formation of filaments with a mixture of divided and non-divided septa (Fig. 2.B). In a similar study, *L. monocytogenes* mutant cells lacking the rodA protein were observed to have shorter cell length (1.3 μm) compared to their wild-type strain (1.9 μm), emphasizing the important role of the *rodA* gene in maintaining the rod shape (Rismondo et al., 2019). Two hypotheses have been proposed to explain the elongation of cells as the result of upregulation of the *rodA* gene and downregulation of the *ftsW* gene. An increase in the concentration of RodA leads to the scarcity of proteins required at the cell division site and hence results in overproduction of peptidoglycan on the lateral wall. The second one is that the overproduction of the RodA protein inhibits the ftsW protein needed for cell division at the site, leading to elongated cells (Rismondo et al., 2019). In another study, downregulation of the cell division gene *ftsX* was observed along with filamentation as the result of salinity stress (2.35 % NaCl) after 30 days of storage (Liu, Miller, et al., 2014). Additionally, this gene was found to be upregulated when the cell filaments started dividing, observed at 60 and 90 days (Liu, Miller, et al., 2014). The downregulation of cell division genes indicates adaptation to stressful conditions, as observed in the study regarding L. *monocytogenes* adaptation to a sublethal dose of carnocyclin A (Liu, Basu, et al., 2014). The cell division protein FtsW regulates the genes *ftsW,* which control the cell division transport system permease protein. Additionally, the *rodA* gene determines the rod shape and the cell division protein in L. *monocytogenes* (Liu, Basu, et al., 2014). The role of ftsW and rodA proteins for the cell shape and morphology has previously been observed for many bacteria, such as *B. subtilis* (Henriques et al., 1998), *E. coli* (Boyle et al., 1997), and *S. pneumoniae.*

While this study focuses on the multispecies biofilm formation on the stainless steel coupon owing to its widespread use in the food industry, the food industry also uses many different types of materials, polytetrafluoroethylene (PTFE) (Giao & Keevil, 2013), ethylene propylene diene monomer rubber (EPDM) (Prabhukhot, Eggleton, Vinyard, & Patel, 2024), polystyrene (Maggio et al., 2021) which were not studied here. Although both static and dynamic flow were studied in 10 % TSB, studies need to be conducted to confirm if similar interactions between *P. fluorescens* and L. *monocytogenes* occur in the presence of flow in nutrient-rich or nutrient-limiting conditions.

5. Conclusion

The stress adaptation of pathogens has been studied extensively in planktonic cells. This study investigated the stress adaptation of L. *monocytogenes* in single and dual-species biofilms with morphological and genetic observations under shear stress. The adaptation of L. *monocytogenes* under shear stress was found to be significantly different in single-species biofilm compared to dual-species (with *P. fluorescens*), indicating the importance of considering multispecies in stress response. The gene expression analysis of cells at 48 h incubation time showed that the cells had already adapted to the hydrodynamic stress, possibly aided by the constant inflow of fresh nutrients in the bioreactor, as indicated by the downregulation of the stress gene *sigB* relative to static conditions (Fig. 6). Another important observation was the filamentation of the bacteria as the result of stress adaptation in a single species (Fig. 2B), which has been associated with the underestimation of cells in the food chain, posing a critical food safety risk (Yamaki et al., 2021). The elongation of cells and formation of filaments in L. *monocytogenes* have been associated with the variation in susceptibility to antimicrobials (Rismondo et al., 2019). This is crucial information to understand the

behaviour of the pathogen L. *monocytogenes* on food processing surfaces under different stressors.

CRediT authorship contribution statement

Krisha Pant: Writing – original draft, Investigation, Formal analysis, Conceptualization. **Jon Palmer:** Writing – review & editing, Supervision, Methodology, Conceptualization. **Steve Flint:** Writing – review & editing, Supervision, Resources, Project administration, Methodology.

Declaration of competing interest

The authors declare that they have no known competing financial interests or personal relationships that could have appeared to influence the work reported in this paper.

Data availability

Data will be made available on request.

References

Alabdullatif, M. (2024). Evaluating the effects of temperature and agitation on biofilm formation of bacterial pathogens isolated from raw cow milk. *BMC Microbiology, 24* (1), 251. https://doi.org/10.1186/s12866-024-03403-4

Al-Sharify, Z. T., Al-Najjar, S. Z., Naser, Z. A., Alsherfy, Z. A. I., & Onyeaka, H. (2025). The impact of fluid flow on microbial growth and distribution in food processing systems. *Foods, 14*(3), 401. https://doi.org/10.3390/foods14030401

Bereksi, N., Gavini, F., Benezech, T., & Faille, C. (2002). Growth, morphology and surface properties of *Listeria monocytogenes* Scott a and LO28 under saline and acid environments. *Journal of Applied Microbiology, 92*(3), 556–565. https://doi.org/10.1046/j.1365-2672.2002.01564.x

Boyle, D. S., Khattar, M. M., Addinall, S. G., Lutkenhaus, J., & Donachie, W. D. (1997). *ftsW* is an essential cell-division gene in *Escherichia coli*. *Molecular Microbiology, 24* (6), 1263–1273. https://doi.org/10.1046/j.1365-2958.1997.4091773.x

Byun, K.-H., Han, S. H., Choi, M. W., Kim, B.-H., & Ha, S.-D. (2024). Efficacy of disinfectant and bacteriophage mixture against planktonic and biofilm state of *Listeria monocytogenes* to control in the food industry. *International Journal of Food Microbiology, 413*, Article 110587. https://doi.org/10.1016/j.ijfoodmicro.2024.110587

Chae, M. S., & Schraft, H. (2000). Comparative evaluation of adhesion and biofilm formation of different *Listeria monocytogenes* strains. *International Journal of Food Microbiology, 62*(1–2), 103–111. https://doi.org/10.1016/S0168-1605(00)00406-2

Cherifi, T., Jacques, M., Quessy, S., & Fravalo, P. (2017). Impact of nutrient restriction on the structure of *Listeria monocytogenes* biofilm grown in a microfluidic system. *Frontiers in Microbiology, 8*, 864. https://doi.org/10.3389/fmicb.2017.00864

Cunault, C., Faille, C., Bouvier, L., Föste, H., Augustin, W., Scholl, S., Debreyne, P., & Benezech, T. (2015). A novel set-up and a CFD approach to study the biofilm dynamics as a function of local flow conditions encountered in fresh-cut food processing equipments. *Food and Bioproducts Processing, 93*, 217–223. https://doi.org/10.1016/j.fbp.2014.07.005

Dong, Q., Sun, L., Fang, T., Wang, Y., Li, Z., Wang, X., Wu, M., & Zhang, H. (2022). Biofilm formation of *Listeria monocytogenes* and *Pseudomonas aeruginosa* in a simulated chicken processing environment. *Foods, 11*(13), 1917. https://doi.org/10.3390/foods11131917

Fagerlund, A., Langsrud, S., & Møretrø, T. (2021). Microbial diversity and ecology of biofilms in food industry environments associated with *Listeria monocytogenes* persistence. *Current Opinion in Food Science, 37*, 171–178. https://doi.org/10.1016/j.cofs.2020.10.015

Fan, Y., Qiao, J., Lu, Z., Fen, Z., Tao, Y., Lv, F., Zhao, H., Zhang, C., & Bie, X. (2020). Influence of different factors on biofilm formation of *Listeria monocytogenes* and the regulation of *cheY* gene. *Food Research International, 137*, Article 109405. https://doi.org/10.1016/j.foodres.2020.109405

Flemming, H.-C., Wingender, J., Szewzyk, U., Steinberg, P., Rice, S. A., & Kjelleberg, S. (2016). Biofilms: An emergent form of bacterial life. *Nature Reviews Microbiology, 14* (9), 563–575. https://doi.org/10.1038/nrmicro.2016.94

Gao, B., Cai, H., Xu, B., Yang, F., Dou, X., Dong, Q., Yan, H., Bu, X., & Li, Z. (2024). Growth, biofilm formation, and motility of *Listeria monocytogenes* strains isolated from food and clinical samples located in Shanghai (China). *Food Research International, 184*, Article 114232. https://doi.org/10.1016/j.foodres.2024.114232

Gao, H., & Liu, C. (2014). Biochemical and morphological alteration of *Listeria monocytogenes* under environmental stress caused by chloramine-T and sodium hypochlorite. *Food Control, 46*, 455–461. https://doi.org/10.1016/j.foodcont.2014.05.016

Giao, M., & Keevil, C. (2013). Hydrodynamic shear stress to remove *Listeria monocytogenes* biofilms from stainless steel and polytetrafluoroethylene surfaces. *Journal of Applied Microbiology, 114*(1), 256–265. https://doi.org/10.1111/jam.12032

Giotis, E. S., Blair, I. S., & McDowell, D. A. (2007). Morphological changes in *Listeria monocytogenes* subjected to sublethal alkaline stress. *International Journal of Food Microbiology, 120*(3), 250–258. https://doi.org/10.1016/j.ijfoodmicro.2007.08.036

Gu, T., Luo, Y., Jia, Z., Meesrison, A., Lin, S., Ventresca, I. J., … Yang, M. (2024). Surface topography and chemistry of food contact substances, and microbial nutrition affect pathogen persistence and symbiosis in cocktail *Listeria monocytogenes* biofilms. *Food Control, 161*, Article 110391. https://doi.org/10.1016/j.foodcont.2014.05.016

Guerreiro, D. N., Wu, J., Dessaux, C., Oliveira, A. H., Tiensuu, T., Gudynaite, D., … Johansson, J. (2020). Mild stress conditions during laboratory culture promote the proliferation of mutations that negatively affect sigma B activity in *Listeria monocytogenes*. *Journal of Bacteriology, 202*(9). https://doi.org/10.1128/jb.00751-19

Habimana, O., Guillier, L., Kulakauskas, S., & Briandet, R. (2011). Spatial competition with *Lactococcus lactis* in mixed-species continuous-flow biofilms inhibits *Listeria monocytogenes* growth. *Biofouling, 27*(9), 1065–1072. https://doi.org/10.1080/08927014.2011.626124

Habimana, O., Meyrand, M., Meylheuc, T., Kulakauskas, S., & Briandet, R. (2009). Genetic features of resident biofilms determine attachment of *Listeria monocytogenes*. *Applied and Environmental Microbiology, 75*(24), 7814–7821. https://doi.org/10.1128/AEM.01333-09

Henriques, A. O., Glaser, P., Piggot, P. J., & Moran, C. P., Jr. (1998). Control of cell shape and elongation by the *rodA* gene in *Bacillus subtilis*. *Molecular Microbiology, 28*(2), 235–247. https://doi.org/10.1046/j.1365-2958.1998.00766.x

Ibusquiza, P. S., Herrera, J. J., Vázquez-Sánchez, D., & Cabo, M. L. (2012). Adherence kinetics, resistance to benzalkonium chloride, and microscopic analysis of mixed biofilms formed by *Listeria monocytogenes* and *Pseudomonas putida*. *Food Control, 25* (1), 202–210. https://doi.org/10.1016/j.foodcont.2011.10.002

Jiang, L., Yue, Y., Zhong, K., Wu, Y., & Gao, H. (2025). Antibiofilm mechanism of pyrrole-2-carboxylic acid by impairing flagellar motility of *Listeria monocytogenes* and its application in cheese. *Food Control, 168*, Article 110974. https://doi.org/10.1016/j.foodcont.2024.110974

Jones, T. H., Vail, K. M., & McMullen, L. M. (2013). Filament formation by foodborne bacteria under sublethal stress. *International Journal of Food Microbiology, 165*(2), 97–110. https://doi.org/10.1016/j.ijfoodmicro.2013.05.001

Jydegaard-Axelsen, A. M., Aaes-Jørgensen, A., Koch, A. G., Jensen, J. S., & Knøchel, S. (2005). Changes in growth, rRNA content, and cell morphology of *Listeria monocytogenes* induced by CO2 up-and downshift. *International journal of food microbiology, 98*(2), 145–155. https://doi.org/10.1016/j.ijfoodmicro.2004.05.019

Kale, S. B., Doijad, S. P., Poharkar, K. V., Garg, S., Pathak, A. D., Raorane, A. V., … Barbuddhe, S. B. (2017). Elucidation of the role of the *minC* gene in filament formation by *Listeria monocytogenes* under stress conditions. *International Journal of Current Research and Review, 9*, 10. https://doi.org/10.7324/IJCRR.2017.99913

Karasz, D. C., Weaver, A. I., Buckley, D. H., & Wilhelm, R. C. (2022). Conditional filamentation as an adaptive trait of bacteria and its ecological significance in soils. *Environmental Microbiology, 24*(1), 1–17. https://doi.org/10.1111/1462-2920.15871

Kocot, A. M., & Olszewska, M. A. (2020). Interaction of *Pseudomonas aeruginosa* and *Staphylococcus aureus* with *Listeria innocua* in dual species biofilms and inactivation following disinfectant treatments. *Lwt, 118*, Article 108736. https://doi.org/10.1016/j.lwt.2019.108736

Li, T., Wang, D., Liu, N., Ma, Y., Ding, T., Mei, Y., & Li, J. (2018). Inhibition of quorum sensing-controlled virulence factors and biofilm formation in *Pseudomonas fluorescens* by cinnamaldehyde. *International Journal of Food Microbiology, 269*, 98–106. https://doi.org/10.1016/j.ijfoodmicro.2018.01.023

Liu, X., Basu, U., Miller, P., & McMullen, L. M. (2014). Stress response and adaptation of *Listeria monocytogenes* 08-5923 exposed to a sublethal dose of carnocyclin a. *Applied and Environmental Microbiology, 80*(13), 3835–3841. https://doi.org/10.1128/AEM.00350-14

Liu, X., Miller, P., Basu, U., & McMullen, L. M. (2014). Sodium chloride-induced filamentation and alternative gene expression of *fts*, *murZ*, and *gnd* in *Listeria monocytogenes* 08-5923 on vacuum-packaged ham. *FEMS Microbiology Letters, 360* (2), 152–156. https://doi.org/10.1111/1574-6968.12599

Livak, K. J., & Schmittgen, T. D. (2001). Analysis of relative gene expression data using real-time quantitative PCR and the 2− ΔΔCT method. *methods, 25*(4), 402–408. https://doi.org/10.1006/meth.2001.1262

Maggio, F., Rossi, C., Chaves-López, C., Serio, A., Valbonetti, L., Pomilio, F., … Paparella, A. (2021). Interactions between *L. monocytogenes* and *P. Fluorescens* in dual-species biofilms under simulated dairy processing conditions. *Foods, 10*(1), 176. https://doi.org/10.3390/foods10010176

Melian, C., Bentencourt, E., Castellano, P., Ploper, D., Vignolo, G., & Mendoza, L. M. (2022). Biofilm genes expression of *Listeria monocytogenes* exposed to *Latilactobacillus curvatus* bacteriocins at 10° C. *International Journal of Food Microbiology, 370*, Article 109648. https://doi.org/10.1016/j.ijfoodmicro.2022.109648

Mendez, E., Walker, D. K., Vipham, J., & Trinetta, V. (2020). The use of a CDC biofilm reactor to grow multi-strain *Listeria monocytogenes* biofilm. *Food Microbiology, 92*, Article 103592. https://doi.org/10.1016/j.fm.2020.103592

Miladi, H., Ammar, E., Ben Slama, R., Sakly, N., & Bakhrouf, A. (2013). Influence of freezing stress on morphological alteration and biofilm formation by *Listeria monocytogenes*: Relationship with cell surface hydrophobicity and membrane fluidity. *Archives of Microbiology, 195*, 705–715. https://doi.org/10.1007/s00203-013-0921-7

Niboucha, N., Goetz, C., Sanschagrin, L., Fontenille, J., Fliss, I., Labrie, S., & Jean, J. (2022). Comparative study of different sampling methods of biofilm formed on stainless-steel surfaces in a CDC biofilm reactor. *Frontiers in Microbiology, 13*, Article 892181. https://doi.org/10.3389/fmicb.2022.892181

Pang, X., & Yuk, H.-G. (2019). Effects of the colonization sequence of *Listeria monocytogenes* and *Pseudomonas fluorescens* on survival of biofilm cells under food-

related stresses and transfer to salmon. *Food Microbiology, 82*, 142–150. https://doi.org/10.1016/j.fm.2019.02.002

Papaioannou, E., Giaouris, E. D., Berillis, P., & Boziaris, I. S. (2018). Dynamics of biofilm formation by *Listeria monocytogenes* on stainless steel under mono-species and mixed-culture simulated fish processing conditions and chemical disinfection challenges. *International Journal of Food Microbiology, 267*, 9–19. https://doi.org/10.1016/j.ijfoodmicro.2017.12.020

Perni, S., Jordan, S. J., Andrew, P. W., & Shama, G. (2006). Biofilm development by *Listeria innocua* in turbulent flow regimes. *Food Control, 17*(11), 875–883. https://doi.org/10.1016/j.foodcont.2005.06.002

Poimenidou, S. V., Caccia, N., Paramithiotis, S., Hébraud, M., Nychas, G.-J., & Skandamis, P. N. (2023). Influence of temperature on regulation of key virulence and stress response genes in *Listeria monocytogenes* biofilms. *Food Microbiology, 111*, Article 104190. https://doi.org/10.1016/j.fm.2022.104190

Prabhukhot, G. S., Eggleton, C. D., Kim, M., & Patel, J. (2024). Impact of surface topography and hydrodynamic flow conditions on single and multispecies biofilm formation by *Escherichia coli* O157: H7 and *Listeria monocytogenes* in presence of promotor bacteria. *Lwt, 116240*. https://doi.org/10.1016/j.lwt.2024.116240

Prabhukhot, G. S., Eggleton, C. D., Vinyard, B., & Patel, J. (2024). Using bio-inline reactor to evaluate sanitizer efficacy in removing dual-species biofilms formed by *Escherichia coli* O157: H7 and *Listeria monocytogenes*. *Journal of Food Protection.* , Article 100314. https://doi.org/10.1016/j.jfp.2024.100314

Puga, C., Orgaz, B., Muñoz, S., & SanJose, C. (2015). Cold stress and presence of *Pseudomonas fluorescens* affect *Listeria monocytogenes* biofilm structure and response to chitosan. *Molecular Genetic Medicine, 9*, 1–6.

Puga, C. H., Dahdouh, E., SanJose, C., & Orgaz, B. (2018). *Listeria monocytogenes* colonizes *Pseudomonas fluorescens* biofilms and induces matrix over-production. *Frontiers in Microbiology, 9*, 1706. https://doi.org/10.3389/fmicb.2018.01706

Redding, M., Zheng, J., Mowery, J., Gu, G., Bolten, S., Luo, Y., & Nou, X. (2024). Microscopic and transcriptomic characterization of *Listeria monocytogenes* aggregation and biofilm formation in cantaloupe juice. *Food Control, 158*, Article 110243. https://doi.org/10.1016/j.foodcont.2023.110243

Rieu, A., Briandet, R., Habimana, O., Garmyn, D., Guzzo, J., & Piveteau, P. (2008). *Listeria monocytogenes* EGD-e biofilms: no mushrooms but a network of knitted chains. *Applied and environmental microbiology, 74*(14), 4491–4497. https://doi.org/10.1128/AEM.00255-08

Rismondo, J., Halbedel, S., & Gründling, A. (2019). Cell shape and antibiotic resistance are maintained by the activity of multiple *FtsW* and *RodA* enzymes in *Listeria monocytogenes*. *MBio, 10*(4). https://doi.org/10.1128/mbio.01448-19

Rodriguez, A., Autio, W. R., & Mclandsborough, L. A. (2008). Effect of surface roughness and stainless steel finish on *Listeria monocytogenes* attachment and biofilm formation. *Journal of Food Protection, 71*(1), 170–175. https://doi.org/10.4315/0362-028X-71.1.170

Santos, T., Viala, D., Chambon, C., Esbelin, J., & Hébraud, M. (2019). *Listeria monocytogenes* biofilm adaptation to different temperatures seen through shotgun proteomics. *Frontiers in Nutrition, 6*, 89. https://doi.org/10.3389/fnut.2019.00089

Sasahara, K. C., & Zottola, E. A. (1993). Biofilm formation by *Listeria monocytogenes* utilizes a primary colonizing microorganism in flowing systems. *Journal of Food Protection, 56*(12), 1022–1028. https://doi.org/10.4315/0362-028X-56.12.1022

Schmid, B., Klumpp, J., Raimann, E., Loessner, M. J., Stephan, R., & Tasara, T. (2009). Role of cold shock proteins in growth of *Listeria monocytogenes* under cold and osmotic stress conditions. *Applied and Environmental Microbiology, 75*(6), 1621–1627. https://doi.org/10.1128/AEM.02154-08

Shah, M., & Bergholz, T. (2020). Variation in growth and evaluation of cross-protection in *Listeria monocytogenes* under salt and bile stress. *Journal of Applied Microbiology, 129*(2), 367–377. https://doi.org/10.1111/jam.14607

Simões, L. C., Gomes, I., Sousa, H., Borges, A., & Simões, M. (2022). Biofilm formation under high shear stress increases resilience to chemical and mechanical challenges. *Biofouling, 38*(1), 1–12. https://doi.org/10.1080/08927014.2021.2006189

Skowron, K., Wiktorczyk, N., Grudlewska, K., Kwiecińska-Piróg, J., Wałecka-Zacharska, E., Paluszak, Z., & Gospodarek-Komkowska, E. (2019). Drug-susceptibility, biofilm-forming ability and biofilm survival on stainless steel of *Listeria* spp. strains isolated from cheese. *International Journal of Food Microbiology, 296*, 75–82. https://doi.org/10.1016/j.ijfoodmicro.2019.02.021

Szlavik, J., Paiva, D. S., Mørk, N., van den Berg, F., Verran, J., Whitehead, K., … Nielsen, D. S. (2012). Initial adhesion of *Listeria monocytogenes* to solid surfaces under liquid flow. *International Journal of Food Microbiology, 152*(3), 181–188. https://doi.org/10.1016/j.ijfoodmicro.2011.09.006

Takahashi, H., Suda, T., Tanaka, Y., & Kimura, B. (2010). Cellular hydrophobicity of *Listeria monocytogenes* involves initial attachment and biofilm formation on the surface of polyvinyl chloride. *Letters in Applied Microbiology, 50*(6), 618–625. https://doi.org/10.1111/j.1472-765X.2010.02842.x

Teh, K. H., Flint, S., Palmer, J., Andrewes, P., Bremer, P., & Lindsay, D. (2014). Biofilm–an unrecognised source of spoilage enzymes in dairy products? *International Dairy Journal, 34*(1), 32–40. https://doi.org/10.1016/j.idairyj.2013.07.002

Utratna, M., Cosgrave, E., Baustian, C., Ceredig, R. H., & O'Byrne, C. P. (2014). Effects of growth phase and temperature on *σB* activity within a *Listeria monocytogenes* population: Evidence for RsbV-independent activation of *σB* at refrigeration temperatures. *BioMed Research International, 2014*(1), Article 641647. https://doi.org/10.1155/2014/641647

Vazquez-Armenta, F., Hernandez-Oñate, M., Martinez-Tellez, M., Lopez-Zavala, A., Gonzalez-Aguilar, G., Gutierrez-Pacheco, M., & Ayala-Zavala, J. (2020). Quercetin repressed the stress response factor (*sigB*) and virulence genes (*prfA*, *actA*, *inlA*, and *inlC*), lower the adhesion, and biofilm development of *L. monocytogenes*. *Food Microbiology, 87*, Article 103377. https://doi.org/10.1016/j.fm.2019.103377

Vázquez-Boland, J. A., Kuhn, M., Berche, P., Chakraborty, T., Dominguez-Bernal, G., Goebel, W., … Kreft, J. R. (2001). *Listeria* pathogenesis and molecular virulence determinants. *Clinical Microbiology Reviews, 14*(3), 584–640. https://doi.org/10.1128/cmr.14.3.584-640.2001

van der Veen, S., & Abee, T. (2010). Importance of *SigB* for *Listeria monocytogenes* static and continuous-flow biofilm formation and disinfectant resistance. *Applied and Environmental Microbiology, 76*(23), 7854–7860. https://doi.org/10.1128/AEM.01519-10

Wang, H., Feng, M., Anwar, T. M., Chai, W., Ed-Dra, A., Kang, X., … Li, Y. (2023). Change in antimicrobial susceptibility of *Listeria* spp. in response to stress conditions. *Frontiers in Sustainable Food Systems, 7*, Article 1179835. https://doi.org/10.3389/fsufs.2023.1179835

Wang, Y., Sun, L., Hu, L., Wang, Z., Wang, X., & Dong, Q. (2022). Adhesion and kinetics of biofilm formation and related gene expression of *Listeria monocytogenes* in response to nutritional stress. *Food Research International, 156*, Article 111143. https://doi.org/10.1016/j.foodres.2022.111143

Wiktorczyk-Kapischke, N., Skowron, K., Grudlewska-Buda, K., Wałecka-Zacharska, E., Korkus, J., & Gospodarek-Komkowska, E. (2021). Adaptive response of *Listeria monocytogenes* to the stress factors in the food processing environment. *Frontiers in Microbiology, 12*, Article 710085. https://doi.org/10.3389/fmicb.2021.710085

Wiktorczyk-Kapischke, N., Skowron, K., Wałecka-Zacharska, E., Grudlewska-Buda, K., Wnuk, K., Buszko, K., & Gospodarek-Komkowska, E. (2023). Assessment of the influence of selected stress factors on the growth and survival of *Listeria monocytogenes*. *BMC Microbiology, 23*(1), 27. https://doi.org/10.1186/s12866-023-02766-4

Yamaki, S., Kawai, Y., & Yamazaki, K. (2021). Long filamentous state of *Listeria monocytogenes* induced by sublethal sodium chloride stress poses risk of rapid increase in colony-forming units. *Food Control, 124*, Article 107860. https://doi.org/10.1016/j.foodcont.2020.107860

Zhou, G., Dong, P., Luo, X., Zhu, L., Mao, Y., Liu, Y., & Zhang, Y. (2024). Combined effects of cold and acid on dual-species biofilms of *Pseudomonas fluorescens* and *Listeria monocytogenes* under simulated chilled beef processing conditions. *Food Microbiology, 117*, Article 104394. https://doi.org/10.1016/j.fm.2023.104394

Zhu, Q., Gooneratne, R., & Hussain, M. A. (2017). *Listeria monocytogenes* in fresh produce: Outbreaks, prevalence and contamination levels. *Foods, 6*(3), 21. https://doi.org/10.3390/foods6030021